Modeling of hollow formation and its dynamics in liquid gas assisted injection molding process

Dong-Hak Kim[1] and Kyung Hyun Ahn*

School of chemical engineering, Seoul National University, Seoul 151-744, Korea
[1]*Department of chemical engineering, Soonchunhyang university, Asan 336-745, Korea*

Abstract

Application of gas assisted injection molding has been expanded during last two decades because of many advantages such as design flexibility, dimensional stability, reduction of machine tonnages, and so on. However, the surface defects including hesitation mark and gloss difference are observed for thick parts. Difficulties in lay-out of the gas channel and processing condition are another disadvantages. Liquid gas assisted injection molding (LGAIM), in which a liquid with a boiling point lower than the temperature of the polymer melt is injected into the melt stream, and travels with the melt into the mold where it vaporizes and pushes the melt downstream and against the cavity walls to create hollow channels within the part, is a good alternative of the conventional gas assisted injection molding especially in manufacturing simple and very thick parts. Though this is a new frontier of the innovation in the injection molding industry, there is no guideline for the design and processing conditions. In this paper, theoretical analysis has been made to describe the hollow formation dynamics in LGAIM. This model provides an insight into LGAIM process: explains why LGAIM has advantages over conventional gas assisted injection molding, and gives a guideline for the design and processing conditions.

Keywords : injection molding, surface defect, gas penetration, gas-assisted, gas dynamics

1. Introduction

Injection molding process has been widely used for manufacturing plastic parts of complex shape. It is especially suitable for mass production because the conversion of the raw material to a finished part usually requires only one operation (Michaeli *et al.*, 1995). Little or no finishing is required and even complicated geometries can be manufactured in a single operation (Michaeli *et al.*, 1995). Despite these advantages, it experiences difficulties such as sink mark or warpage especially in the production of parts with thick walls (Kim, 1996; Kim and Ahn, 1998; Ahn and Kim, 1998). For example, the sink mark that occurs due to volume contraction of the plastic cannot be completely compensated by the subsequent inflow of melt, which results in defects of the final products. To get over these difficulties, new molding processes have been continuously developed. The gas assisted injection molding process is one of them, which has been survived and proliferated for the last several years. In this process, high pressure gas is injected into the interior of the melt with the objective of compensating volume contraction during the cooling pro-

cess. The gas produces a bubble which pushes the melt into the extremities of the mold creating hollow sections as the bubble propagates. With this process, moldings can be produced free of sink mark with other advantages. It increases design flexibility as well as productivity allowing thick sections in the part design like large ribs or flow leaders, high stiffness to weight ratio in structured parts, lower clamp tonnage and lower injection pressure, reduced cycle time, good dimensional stability with reduced stress distribution, to list a few (Shen, 2001; Chen and Cheng, 1996; Chao *et al.*, 1999; Parvez *et al.*, 2002). It is not easy, in general, to control gas flow as it is very sensitive to processing conditions, and it is very important to control gas flow and to lay out the gas channel in part design (Stevenson, 1996). However, there still exist some disadvantages mainly arising from the difficulties in the control of gas flow, and several variations of gas assisted injection molding have been developed to overcome these limitations. One of them is the liquid gas assisted injection molding (LGAIM) process.

In the liquid gas assisted injection molding process, a liquid with a boiling point lower than the temperature of the polymer melt is injected into the melt stream, and travels with the melt into the mold where it vaporizes and pushes the melt downstream and against the cavity walls to create

hollow channels within the part (Stevenson, 1996). In conventional gas assisted injection molding, high pressure inert gas is injected into the melt, which makes it difficult to control gas flow. However, in LGAIM process, as a small amount of liquid is injected, and it vaporizes and forms a hollow section as it moves with the melt, it does not require high pressure gas and it is relatively easy to control gas flow. By controlling the position and the amount of liquid injected, it is possible to control the void fraction of the molded part. It eliminates sink mark as the vaporized pressure functions as a hold pressure, and it also eliminates another surface defect, hesitation mark, which arises from the cooling of melt front at the onset of gas injection just after the short shot. Though LGAIM is a new frontier of the innovation in the injection molding industry, there has been no guideline for the design and processing conditions. In this paper, theoretical analysis has been made to describe the hollow formation dynamics in LGAIM as well as to provide a guideline for the design and processing conditions.

2. Preliminary estimates of maximum pressure and volume

2.1. Maximum pressure

In the liquid gas assisted injection, volatile liquid is injected into the melt at an appropriate time during the filling process. The liquid absorbs latent heat from the surrounding melt, evaporates and expands. In order to estimate the maximum pressure of the vapor produced in this process, we assume that the liquid rapidly evaporates and reaches the melt temperature instantaneously, which means that heat transfer is very fast and the vapor reaches the melt temperature instantaneously keeping the liquid volume constant. Then the vapor pressure will be very high, and this becomes a driving force for the gas penetration.

If the liquid volume injected is V_o, the liquid evaporates instantaneously keeping the volume constant, and the vapor temperature reaches the melt temperature. If the gas is ideal, vapor pressure is

$$P_g V_g = nR\ T_g \tag{1}$$

where V_g and T_g are volume and temperature of the vapor, respectively. We assume that V_g is V_o, and T_g is the melt temperature T_p. R is a gas constant, and n is the mol number of the vapor. As n is equivalent to the mol number of liquid injected,

$$n = \frac{m}{M} = \frac{\rho_l V_0}{M} \tag{2}$$

Here, ρ_l is the density of the liquid, and M is the molecular weight.

From Eq (1) and (2), the vapor pressure is

$$P_g = \frac{nRT_p}{V_0} = \frac{\rho_l RT_p}{M} \tag{3}$$

If the melt temperature is 200°C and water is injected at room temperature, then

$$P_g = \frac{1g/cm^3 0.082\ l \cdot atm/mol \cdot K 473K}{18g/mol} \frac{1000cm^3}{1\ l} = 2155\ atm \tag{4}$$

To make the estimation more precise, we now use the equation of state of a real gas, the compressibility factor equation of state. As the critical pressure and temperature of water is 218.3 atm and 647.4 K, respectively, and the vapor evaporates keeping the volume constant, the reduced temperature and pressure becomes

$$T_r = \frac{T_p}{T_c} = \frac{473K}{647.4K} = 0.731 \tag{5}$$

$$V_r = \frac{V_{\frac{P_c}{n}}}{RT_c} = \frac{0.018\ l/mol\,218.3\ atm}{0.082\frac{latm}{molK}647.4K} = 0.074 \tag{6}$$

From Perry's handbook, the compressibility factor z can be obtained as $z \doteq 4$. That is, the vapor pressure is roughly 4 times of the pressure calculated in Eq (4), and becomes

$$P_g = z\frac{nRT_p}{V_0} \cong 4*2155 = 8620\ atm \tag{7}$$

From the above estimation with water, it can be known that the instantaneous vapor pressure can be as large as one order higher than that in normal gas assisted injection. It is expected in the real situation that the maximum vapor pressure will be much less than the estimation given above because the assumptions we have used are too simplistic: that is, the gas does not reach the melt temperature instantaneously, the gas volume increases during vaporization, and there exists a resistance of heat transfer leading to a pressure loss. Nevertheless, the vapor pressure will be large enough to push the melt to fill up the mold in a short shot. This can also be experienced by the bursting often observed in the preliminary operations. To calculate the vapor pressure more precisely, an improved analysis of the vaporization mechanism will be necessary. From Eq. (3), it can be noted that the maximum pressure depends on the species of liquid, which means that the selection or the development of appropriate liquid is required depending on the products or the applications.

2.2. Maximum void volume

With the same assumptions, we now estimate the maximum void volume. The vapor formed by evaporation expands in the mold, and finally the gas pressure drops to the pressure in the cavity. If the final pressure in the cavity is assumed to be atmospheric pressure and there is no heat loss during the process of expansion keeping the initial

temperature, then from the ideal equation of state the final vapor volume will be

$$V_{max} = \frac{nRT_p}{P_{atm}} = \frac{\rho_l RT_p}{P_{atm}M}V_0 \tag{8}$$

where P_{atm} is atmospheric pressure. The maximum volume expansion ratio can be estimated by (assuming the liquid is water)

$$\frac{V_{max}}{V_0} = \frac{\rho_l RT_p}{P_{atm}M} = \frac{1*0.082*473*1000}{1*18} = 2155 \tag{9}$$

That is the volume expands as much as about 2000 times. We assumed that there is no heat loss and the liquid expands up to atmospheric pressure without any restriction of the mold. In the actual process, the pressure in the cavity is much higher than the atmospheric pressure, and the temperature of both vapor and melt becomes much lower than the melt temperature due to the cold mold, the volume expansion ratio will be much lower than the above estimation. However, it should be noted that the liquid expands depending not only on the processing conditions such as temperature and pressure but also on the type of liquid.

3. Dynamics in liquid gas assisted injection

Liquid gas assisted injection may be compared with that of gas assisted injection molding. Similarity is that the process is controlled by the gas dynamics whether it is introduced as a pressurized gas from the start or introduced as a liquid but turns into a gas after evaporation. Difference is that controlled high pressure gas is injected during mold filling in the former case, while the pressure gradient is derived by evaporation of an injected liquid in the latter. Pressurized gas is supplied to fill the mold in the former, while significant pressure drop occurs compensating the mold filling in the latter. Even though the mechanism of both processes will be different, there exist some similarity. So we first describe the problem, and investigate the gas dynamics of a conventional gas assisted injection molding (Shen, 2001; Chen and Cheng, 1996; Chao et al., 1999; Poslinski and Stokes, 1993) before we discuss the dynamics of liquid gas assisted injection.

3.1. Problem description

The gas assisted displacement of polymer melt as well as the displacement of the gas is schematically depicted in Fig. 1(Poslinski and Stokes, 1993). The total volume of the melt to be displaced is $\pi R^2 Z_0$, and the vaporized gas at $t = 0$ pushes polymer melt from $z = 0$. The gas pressure at this instant is P_g, the pressure in the cavity is P_0, and the pressure drop is defined as $\Delta p_g = P_g - P_0$. In the figure, U_b is the average velocity of the bubble, U_l is the average velocity of the melt front, ζ is the position of the gas front, Z is the position of the melt front, and δ is the liquid coating
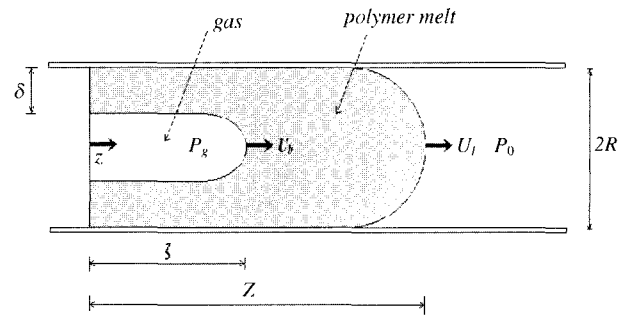

Fig. 1. Schematic diagram for problem description.

thickness which is the thickness of the melt remaining on the wall. Then the fraction of the tube volume ϕ occupied by the melt layer between $z = 0$ and $z = \zeta$ becomes,

$$\phi = \frac{\pi R^2 \zeta - \int_0^\zeta \pi (R-\delta)^2 dz}{\pi R^2 \zeta} = 1 - \frac{1}{\zeta}\int_0^\zeta (1-\varepsilon)^2 dz \tag{10}$$

where the thickness ratio is defined as $\varepsilon = \delta/R$.

In the limiting case of $\delta = 0$, the gas pushes the melt completely and never reaches the advancing melt front. This is only possible when perfect slip exists along the wall, so $\delta > 0$ in general. In this case, the distance between the melt front and the gas front $Z - \zeta$ decreases with time, and a blowout of the gas may happen. The time and position at blowout is defined as $t = t_b$ and $Z = \zeta_b$. In addition, blowout ratio ζ_b/Z_0 characterizes the distance traveled by the melt front relative to its initial axial position.

3.2. Gas dynamics in gas assisted injection

As the volume of the melt traveled by the melt front is equal to the volume of the gas displaced downstream of the gas front,

$$\pi R^2 (Z-Z_0) = \int_0^\zeta \pi (R-\delta)^2 dz. \tag{11}$$

$\varepsilon = \delta/R$ and ε is a function of z in general. Then,

$$Z-Z_0 = \int_0^\zeta [1-\varepsilon(z)]^2 dz. \tag{12}$$

With Eq. (10), it becomes

$$Z - Z_0 = (1 - \phi)\zeta \tag{13}$$

Then the blowout position $Z = \zeta = \zeta_b$ can be determined in terms of the initial melt length (or equivalently volume) and the coating volume fraction as following

$$\zeta_b = Z_0/\phi. \tag{14}$$

As the average velocity of the melt front and the average velocity of the gas front are defined as $U_l = \frac{dZ}{dt}$, $U_b = \frac{d\zeta}{dt}$, respectively, differentiation of Eq. (12) with respect to time leads to

$$U_l = \frac{d}{dt}\int_0^\zeta [1-\varepsilon(z)]^2 dz = \frac{d\zeta}{dt}\cdot\frac{d}{d\zeta}\int_0^\zeta [1-\varepsilon(z)]^2 dz = U_b[1-\varepsilon(\zeta)]^2$$

$$(15)$$

If the gas could displace all the liquid, then $\varepsilon = 0$, $\phi = 0$, and the displacement between the two fronts $Z - \zeta$ would remain unchanged from its initial value Z_0. Then the melt front and the bubble would travel with the same average velocity, and the blowout would never occur. However, when $\varepsilon > 0$, $\phi > 0$, $Z - \zeta$ diminishes with time and gas penetration rate is higher by a factor of $1/(1-\varepsilon)^2$.

Now, let us make some assumptions. First, the melt is assumed to be Newtonian, and the thickness ratio ε is a constant (ε_∞) independent of time and position. Also the pressure drop ΔP_g is assumed to be constant ($\Delta P_g = P_0$). Then Eq. (12) can be rewritten as

$$Z - Z_0 = (1-\varepsilon_\infty)^2\zeta.$$

$$(16)$$

If we use Hagen-Poisseuille equation of a Newtonian fluid flow, the flow rate becomes

$$Q = \pi R^2 U_l = \frac{\pi R^4 \Delta P_0}{8\mu(Z-\zeta)}$$

$$(17)$$

or

$$(Z-\zeta)U_l = \frac{R^2\Delta P_0}{8\mu}$$

$$(18)$$

If we differentiate Eq. (16) with time,

$$U_l = (1-\varepsilon_\infty)^2\frac{d\zeta}{dt}.$$

$$(19)$$

Inserting this result to Eq. (18),

$$(1-\varepsilon_\infty)^2(Z-\zeta)\frac{d\zeta}{dt} = \frac{R^2\Delta P_0}{8\mu}$$

$$(20)$$

Now let us estimate the initial velocity of the gas front and the blowout time.

As $\zeta = 0, U_b = \frac{d\zeta}{dt} = U_i$ at $t = 0$, Eq. (20) with $Z = Z_0$ becomes

$$U_i = \frac{R^2\Delta P_0}{8\mu Z_0(1-\varepsilon_\infty)^2}.$$

$$(21)$$

When $t = t_b$, or when the gas crosses the melt front, the initial volume of the melt $\pi R^2 Z_0$ is equivalent to the amount remaining on the wall. Then $\pi R^2 Z_0 = [\pi R^2 - \pi(R-\delta)^2]\zeta_b$, and the blowout position of the bubble becomes

$$\zeta_b = \frac{Z_0}{1-(1-\varepsilon_\infty)^2}.$$

$$(22)$$

As $\phi = 1-(1-\varepsilon_\infty)^2$, Eq. (20) becomes

$$(1-\phi)(Z-\zeta)\frac{d\zeta}{dt} = \frac{R^2\Delta P_0}{8\mu}$$

$$(23)$$

and Eq. (16) becomes

$$Z - Z_0 = (1-\phi)\zeta.$$

$$(24)$$

Inserting Eq. (24) into Eq. (23), a differential equation on ζ can be derived and solved with the boundary conditions $t = 0$, $\zeta = 0$ and $t = t_b$, $\zeta = Z_0/\phi$.

$$(1-\phi)\int_0^{\zeta_b}(Z_0-\phi\zeta)d\zeta = \frac{R^2\Delta P_0}{8\mu}\int_0^{t_b}dt$$

$$(1-\phi)\left(Z_0\zeta_b - \frac{\phi}{2}\zeta_b^2\right) = \frac{R^2\Delta P_0}{8\mu}t_b$$

If we use $\zeta_b = \frac{Z_0}{\phi}$, then the blowout time can be obtained as

$$t_b = \left(\frac{1-\phi}{\phi}\right)\left(\frac{4\mu Z_0^2}{R^2\Delta P_0}\right)$$

$$(25)$$

Eq. (21) and (25) show the coupled influence of the process variables on the gas assisted displacement process. For example, a higher viscosity and a large amount of melt to be displaced increases the flow resistance, thereby reducing the bubble velocity and delaying blowout.

If we insert Eq. (24) into Eq. (23), then a differential equation on ζ can be derived as follows

$$(1-\phi)(Z_0-\phi\zeta)d\zeta = \frac{R^2\Delta P_0}{8\mu}dt.$$

$$(26)$$

With the initial condition $t = 0$, $\zeta = 0$, it becomes

$$\frac{1}{2}\phi(1-\phi)\zeta^2 - (1-\phi)Z_0\zeta + \frac{R^2\Delta P_0}{8\mu}t = 0$$

$$(27)$$

and can ben solved for ζ as follows

$$\zeta = \frac{Z_0}{\phi} \pm \frac{Z_0}{\phi}\sqrt{1-\left(\frac{\phi}{1-\phi}\right)\left(\frac{R^2\Delta P_0}{4\mu Z_0^2}\right)t}$$

$$(28)$$

or

$$\frac{\zeta}{\zeta_b} = 1 - \sqrt{1-\frac{t}{t_b}}$$

$$(29)$$

Eq. (29) and (24) can be combined to give

$$\frac{Z}{\zeta_b} = 1 - (1-\phi)\sqrt{1-\frac{t}{t_b}}$$

$$(30)$$

If we differentiate Eq. (29) and (30) with respect to time, then the velocity of the gas front and the velocity of the melt front can be obtained as follows

$$\frac{U_b}{U_i} = \frac{1}{\sqrt{1-\frac{t}{t_b}}}$$

$$(31)$$

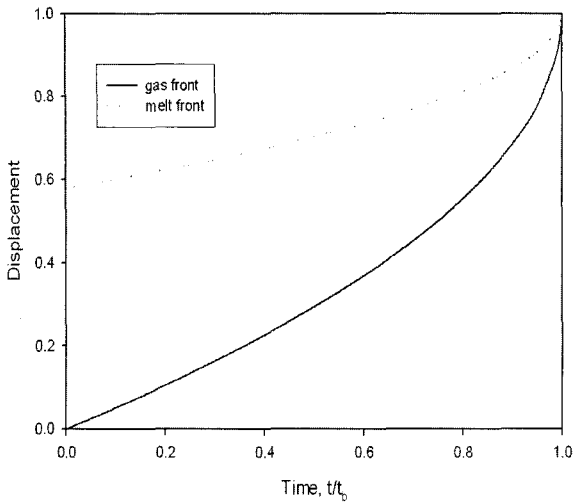$$\frac{U_l}{U_i} = \frac{1-\phi}{\sqrt{1-\frac{t}{t_b}}}.$$

$$(32)$$

30

Fig. 2. Displacement of gas front and melt front as a function of time in a conventional gas assisted injection molding.
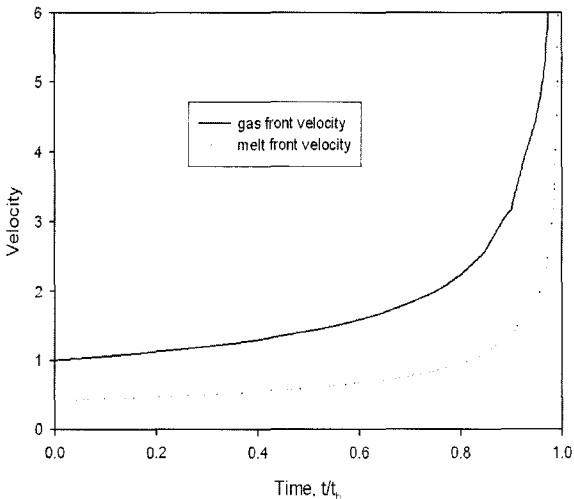

Fig. 3. Velocity of gas front and melt front as a function of time in a conventional gas assisted injection molding.

The predictions of these results are given in Fig. 2 and Fig. 3.(assuming the Newtonian fluid, $\varepsilon_\infty = 0.35$) As shown in the figures, when the gas penetrates the melt maintaining the pressure to be constant, the amount of melt between the melt front and the gas front diminishes as time goes on, and the flow resistance becomes reduced, leading to an acceleration of the gas front. So the velocity of the gas front increases dramatically just before the blowout, which is qualitatively in good agreement with experiments (Poslinski and Stokes, 1993).

4. Gas dynamics in liquid gas assisted injection

Unlike the gas assisted injection molding which maintains high pressure of the gas, it is not possible to keep the gas pressure constant in LGAIM, because the pressure

drop decreases as the vaporized gas expands its volume. So, the idea is to take the pressure drop into account as a function of time. As a simple approximation, let us assume that the pressure drop decreases linearly with time.

$$\frac{\Delta P_g}{\Delta P_0} = 1 - \frac{t}{\tau} \tag{33}$$

where τ is a time constant which reflects the rate of pressure drop. If we rewrite the governing equation, Eq. (23), taking Eq. (33) into account,

$$(1-\phi)(Z-\zeta)\frac{d\zeta}{dt} = \frac{R^2 \Delta P_0}{8\mu}\left(1 - \frac{t}{\tau}\right) \tag{34}$$

Inserting Eq. (24) into Eq. (34), a differential equation on ζ can be derived and solved with the boundary conditions $t = 0$, $\zeta = 0$ and $t = t_b$, $\zeta = Z_0/\phi$ to give the blowout time

$$t_b - \frac{t_b^2}{2\tau} = \left(\frac{1-\phi}{\phi}\right)\left(\frac{4\mu Z_0^2}{R^2 \Delta P_0}\right). \tag{35}$$

If we insert Eq. (24) into Eq. (34), then a differential equation on ζ can be derived as follows

$$(1-\phi)(Z_0 - \phi\zeta)d\zeta = \frac{R^2 \Delta P_0}{8\mu}\left(1 - \frac{t}{\tau}\right)dt \tag{36}$$

If we integrate Eq. (36) with the initial condition $t = 0$, $\zeta = 0$, then

$$(1-\phi)\left(Z_0\zeta - \frac{\phi}{2}\zeta^2\right) = \frac{R^2 \Delta P_0}{8\mu}\left(t - \frac{t^2}{2\tau}\right) \tag{37}$$

and solving for ζ leads to

$$\zeta = \frac{Z_0}{\phi} - \frac{Z_0}{\phi}\sqrt{1 - \left(\frac{\phi}{1-\phi}\right)\left(\frac{R^2 \Delta P_0}{4\mu Z_0^2}\right)\left(t - \frac{t^2}{2\tau}\right)} \tag{38}$$

or

$$\frac{\zeta}{\zeta_b} = 1 - \sqrt{1 - \frac{\frac{t}{t_b} - \frac{t_b}{2\tau}\left(\frac{t}{t_b}\right)^2}{1 - \frac{1}{2}\frac{t_b}{\tau}}} \tag{39}$$

As τ is a time constant relating with the rate of the pressure drop, the gas pressure is maintained longer when τ is larger. If we define the blowout time relative to the time constant to be $\alpha = t_b/\tau$, the gas pressure is maintained long enough to keep the displacement of the melt when $\alpha \ll 1$. When $\alpha \approx 1$, the gas pressure drops fast and the driving force to push the melt becomes reduced.

If we combine Eq. (39) and (24),

$$\frac{Z}{\zeta_b} = 1 - (1-\phi)\sqrt{1 - \frac{\frac{t}{t_b} - \frac{\alpha}{2}\left(\frac{t}{t_b}\right)^2}{1 - \frac{\alpha}{2}}}. \tag{40}$$

If Eq. (39) and (40) are differentiated with time

$$\frac{U_b}{U_i} = \left[1 - \frac{\frac{t}{t_b} - \frac{\alpha}{2}\left(\frac{t}{t_b}\right)^2}{1 - \frac{\alpha}{2}} \right]^{-\frac{1}{2}} \qquad (41)$$

and

$$\frac{U_f}{U_i} = \left(1 - \alpha\frac{t}{t_b}\right)(1 - \phi)\left[1 - \frac{\frac{t}{t_b} - \frac{\alpha}{2}\left(\frac{t}{t_b}\right)^2}{1 - \frac{\alpha}{2}} \right]^{-\frac{1}{2}} \qquad (42)$$

When the pressure drop decreases linearly with time due to the expansion of the gas volume as it penetrates the melt, the positions and velocities of the melt front and gas front can be estimated with above equations. The results are
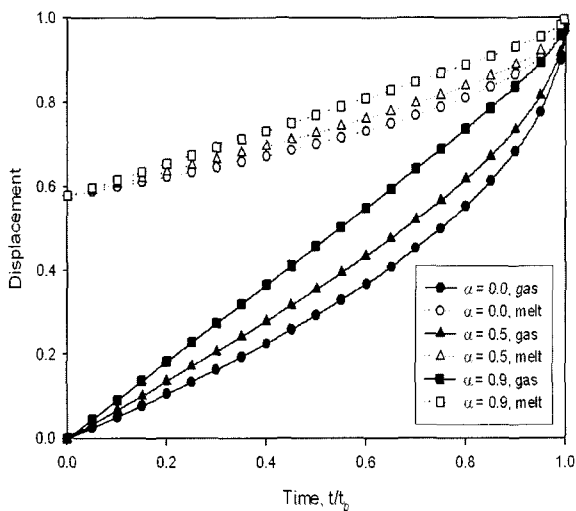

Fig. 4. Displacement of gas front and melt front as a function of time in LGAIM (when is zero, the system becomes the conventional gas assisted injection molding).
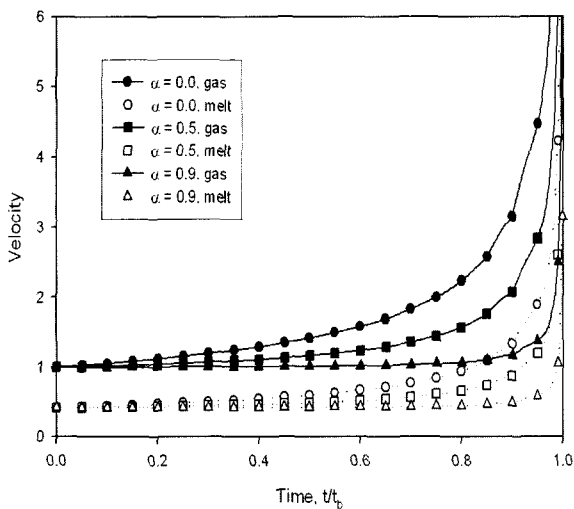

Fig. 5. Velocity of gas front and melt front as a function of time in LGAIM (when is zero, the system becomes the conventional gas assisted injection molding).

given in Fig. 4 and Fig. 5. When α is small, the time constant is large and the gas pressure is maintained. On the other hand, when α is close to one, then the pressure drop decreases with time. When $\alpha = 0.9$, as shown in Fig. 4, the displacement of gas front as well as melt front is larger than the case of lower α. It increases almost linearly with time, contrary to the cases with lower α where it increases very fast as time approaches the blowout time. When $\alpha = 0.9$ as shown in Fig. 5, the velocity of melt front as well as gas front remains almost constant and acceleration is not observed until it reaches very close to the blowout time. When the pressure drop is maintained, the flow resistance decreases and the velocity increases very fast with time as the amount of melt between the melt front and the gas front diminishes. When the pressure drop decreases with time, the flow resistance diminishes due to gas penetration. However, as pressure drop decreases as well in this case, the velocities of the gas front and the melt front do not accelerate and keep constant unless very close to the blowout time. If the acceleration is too fast, a flow mark may occur on the surface of the molded part. It means that it becomes more difficult to control the process as well. As LGAIM inhibits severe acceleration compared to the typical gas assisted injection molding, it has the advantages in both process control and the appearance of the finished product. Our modeling shows the advantages of LGAIM though it is crude and can be regarded as a first estimate.

5. Conclusions

In order to understand the hollow formation as well as the gas assist effect in the mold filling process of LGAIM, the maximum pressure of the vaporized gas as well as the maximum void volume has been estimated. The gas pressure arising from the evaporation of the liquid injected into the melt stream was found to be large enough to push the melt, to fill the mold, and to provide good performance. It was a rough estimate, and the result will not coincide with the experiments quantitatively due to the approximations we have made, but it opens an understanding of this new process. As the flow resistance diminishes due to gas penetration in LGAIM, the pressure drop decreases as processing proceeds, When time constant is small (pressure drop becomes significant to compensate the gas penetration), the displacement of the gas front as well as the melt front increases almost linearly with time, and the velocity of the gas front as well as the melt front remains almost constant during the whole process except close to the blowout time. As there is no acceleration of the velocities of the gas and melt front, it is easier to control the process and also reduces the flow mark often observed in conventional gas assisted injection molding. It means that it has the advantages in both process control and the appearance of

he finished product over the conventional gas assisted injection molding process. In addition to providing an understanding of the process and a guideline for the design and processing, our modeling proves the advantages of LGAIM, though it is crude and can be regarded as a first estimate.

Acknowledgements

Nomenclature

P_g	: pressure of vapor [atm]
V_g	: volume of vapor [l]
n	: mole number of liquid [mol]
R	: ideal gas constant
T_g	: temperature of vapor [K]
P_l	: density of liquid [g/cm^3]
V_0	: initial liquid volume [l]
M	: molecular weight [g/mol]
m	: liquid mass [g]
T_p	: polymer melt temperature [K]
T_c	: critical temperature [K]
P_c	: critical pressure [atm]
T_r	: reduced temperature
V_r	: reduced volume
R	: radius of tube
z	: compressibility factor
V_{max}	: maximum void volume [l]
Z_0	: initial position of melt front
ΔP_g	: pressure drop
U_b	: average bubble velocity
U_l	: average melt front velocity
ζ	: position of gas front
Z	: position of melt front
δ	: residual melt thickness
Φ	: melt fraction in tube between $z = 0$ and $z = \zeta$
ε	: thickness ratio (δ/R)
ε_∞	: critical thickness ratio
t_b	: blowout time
ξ_b	: blowout position
μ	: melt viscosity
U_i	: initial velocity of gas front
τ	: time constant relating with the rate of pressure drop
α	: dimensionless blowout time (t_b/τ)

References

Ahn, Kyung Hyun and Dong-Hak Kim, 1998, Mechanism of the void growth in partial frame process, *Polym. Eng. & Sci.* **38**(10), 1708.

Chao, S.M., S.M. Wang, S.C. Chen and F. Gao, 1999, Evaluation of gas pressure dynamics for gas-assisted injection molding process, *Int. Comm. Heat Mass Transfer* **26**(1), 85.

Chen, S.C. and N.T. Cheng, 1996, A simple model for evaluation of contribution factors to skin melt formation in gas-assisted injection molding, *Int. Comm. Heat Mass Transfer* **23**(2), 215.

Kim, Dong-Hak, 1996, Partial frame process, *Polymer Science and Technology* **7**(3), 303.

Kim, Dong-Hak and Kyung H. Ahn, 1998, Modeling of void growth in partial frame process, *J. of Reinforced Plastics and Composites* **17**(10), 893.

Michaeli, R.C., H. Kaufmann, H. Grief, G. Kretzschmar and R. Bertuleit, 1995, Training in injection molding, Hanser Publishers, Munich Vienna New York.

Parvez, M.A., N.S. Ong, Y.C. Lam and S.B. Tor, 2002, Gas-assisted injection molding: the effects of process variables and gas channel geometry, *J. Mater. Proc. Tech.* **121**, 27.

Polinski, A.J. and V.K. StokesS, 1993, Gas-assisted displacement of a viscous liquid in a tube, *SPE ANTEC Tech. papers* **39**, 68.

Shen, Y.K., 2001, The study on polymer melt front, gas front and solid layer in filling stage of gas-assisted injection molding, *Int. Comm. Heat Mass Transfer* **28**(1), 139.

Stevenson, J.F., 1996, Innovation in polymer processing: Molding, Carl Hanser Verlag.